

ADVANCED 3D LASER MICROSCOPY FOR MEASUREMENTS AND ANALYSIS OF VITRIFIED BONDED ABRASIVE TOOLS

WOJCIECH KAPLONEK, KRZYSZTOF NADOLNY*

Department of Production Engineering, Faculty of Mechanical Engineering, Koszalin
University of Technology, Raclawicka 15-17, 75-620, Koszalin, Poland

*Corresponding Author: krzysztof.nadolny@tu.koszalin.pl

Abstract

In many applications, when a precise non-contact assessment of an abrasive tools' surface is required, alternative measurement methods are often used. Their use offers numerous advantages (referential method) as they introduce new qualities into routinely realized measurements. Over the past few years there has been a dynamic increase in the interest for using new types of classical confocal microscopy. These new types are often defined as 3D laser microscopy. This paper presents select aspects of one such method's application – confocal laser scanning microscopy – for diagnostic analysis of abrasive tools. In addition this paper also looks at the basis for operation, the origins and the development of this measurement technique. The experimental part of this paper presents the select results of tests carried out on grinding wheel active surfaces with sintered microcrystalline corundum grains SGTM bound with glass-crystalline bond. The 3D laser measuring microscopes LEXT OLS3100 and LEXT OLS4000 by Olympus were used in the experiments. Analysis of the obtained measurement data was carried out in dedicated OLS 5.0.9 and OLS4100 2.1 programs, supported by specialist TalyMap Platinum 5.0 software. The realized experiments confirmed the possibility of using the offered measurement method. This concerns both the assessment of grinding wheel active surfaces and their defects, as well as the internal structures of the tools (grain-bond connections). The method presented is an interesting alternative to the typical methods used in the diagnostics of abrasive tools.

Keywords: 3D laser microscopy, Confocal laser scanning microscopy,
Abrasive tools, Grinding wheel, Grinding process.

1. Introduction

Grinding is one of the most widely used material removal machining methods, especially in highly-efficient automated production processes [1, 2]. A number of

Nomenclatures

<i>Ra</i>	arithmetic mean deviation of profile, mm
<i>Rku</i>	kurtosis of profile
<i>Rp</i>	maximum profile peak height, mm
<i>Rq</i>	root mean square deviation of profile, mm
<i>Rsk</i>	skewness of profile
<i>Rt</i>	total height of profile, mm
<i>Rv</i>	maximum profile valley depth, mm
<i>Rz</i>	maximum height of profile, mm
<i>Sa</i>	arithmetic mean height, mm
<i>Sdr</i>	developed interfacial area ratio, %
<i>Sds</i>	density of summits of the surface, 1/mm ²
<i>St</i>	total height of the surface, mm

Abbreviations

CLSM	Confocal Laser Scanning Microscopy
CPA	Circular Pinhole Aperture
CPCG	<i>Continuous Path Controlled Grinding</i>
EMBL	European Molecular Biology Laboratory
GWAS	Grinding Wheel Active Surface
HSG	High Speed Grinding
HSP	High Speed <i>Peelgrinding</i>
MEMS	Micro Electro-Mechanical Systems
SEM	Scanning Electron Microscopy

modern grinding types such as: high speed grinding (HSG) [3], continuous path controlled grinding (CPCG) [4], high speed peelgrinding (HSP) [5], Quickpoint[®] method [6] and single-pass grinding [7] are commonly used within the machine, aerospace and automotive industries. A wide range of abrasive tools are used in these grinding processes [8-10]. One of the most popular tools are grinding wheels with a vitrified bond. They are used in finish machining of surfaces that require a high degree of dimensional and shaped precision, and a good surface layer quality (e.g. relatively slight height of surface unevenness, stress condition favorable for the maintenance of the tool, lack of defects). When such tools are at work, their active surface is often worn off. Such wear manifests itself at the microscale through the blunting of abrasive grain vertexes, and the chipping and smearing of free intergranular spaces with chips of machined material. Whilst at the macroscale this process manifests itself in changes of the circumferential (occurrence of the roundness error) and axial outline of the tool (edge wear). In particular cases progressive wear may result in creation of workpiece surface defects such as grinding burns and microcracks, which may exert significant influence upon the whole machining process [11, 12]. The occurrence of the such effects gave birth to the need for precision assessment and analysis of the abrasive tool active surface condition, particularly for diagnostic purposes.

At present there are a number of measurement methods that make precision assessment possible. Their classification and characteristics were discussed in detail i.e. by Byrne et al. [13] and Tönshoff et al. [14]. The most effective of these

include stylus profilometry [15], optical profilometry [16], interferential microscopy [17] and scanning electron microscopy (SEM) [18].

Other alternative methods used in diagnostics of abrasive tools are modern variations of confocal microscopy defined as 3D laser microscopy [19]. This term includes confocal techniques in which laser radiation and the process of precise surface scanning are utilised. The 3D laser microscopy is particularly identified with confocal laser scanning microscopy (CLSM) [20]. This technique offers a range of unique features such as:

- The possibility of acquiring images of individual slices for subsequent sections, and the generation of spatial images of the examined surface,
- Acquiring high quality images with high depth of field and contrast in a wide range of magnifications up to $\sim 24.000\times$,
- Application of spatial filtering techniques to remove image blurriness and other types of undesirable phenomena such as glare and reflections on the examined surface,
- Non-contact (non-invasive) measurement methods which allow the examination of smooth and super-smooth surfaces, which are usually non-resistant with regard to pollutants, which in turn makes them susceptible to deformations and sensitive to influences of a physical and chemical nature,
- Relatively short measurement and acquisition period with regard to data processing,
- The possibility of measuring the examined surface without the necessity to carry out the time-consuming preparation processes.

In this work the Authors analyzed the possibility of using advanced 3D laser microscopy for measuring and analyzing the condition of the grinding wheel active surface (GWAS) with microcrystalline sintered corundum grains SGTM bound with glass-crystalline bond. Advanced laser microscopes from the LEXT line – OLS3100 and OLS4000 by Japanese Olympus were used in the experiments. They are described in subsequent parts of the work, along with selected results of the measurements and analyses.

2. The Principles and Genesis of the CLSM Technique

Numerous limitations of the classical light microscopy (both transmission and fluorescent) [21] can be observed when applying these methods to research involving surface examinations that require high magnification levels, or high resolutions, of the images obtained. One of the basic limitations is the light that comes from outside the focal plane (that generates an image with varying depth of focus). The light microscope acquires images not only from this plane but also from the whole section of the sample. The images generated in the focal plane are characterized by high depth of field and contrast. The images located outside the plane (before and behind it) are blurred. As a result the image obtained with a classical light microscope is characterized by highly blurred background that decreases the focus of the contours and considerably diminishes the quality of the details observed. Through application of a simple solution, in the form of a circular pinhole aperture, confocal microscopy allows for the elimination of such images, leaving only those that come from the focal plane. The thickness of this plane,

and thus the resolution of the confocal microscopy is usually the function of the pinhole diameter and the length of the incident light wave [22]. Changing the focal plane location also allows for obtaining images of individual slices acquired for subsequent sections. The collection of such images after their proper processing allows for 3D reconstruction of the examined surface.

The theoretical foundations of classical confocal microscopy were developed in the mid 1950's in the United States by M. Minsky (Harvard University). Minsky's works resulted in the construction of the first fully operational double-focusing stage scanning microscope (of his own construction) [23]. This solution was patented at the end of 1961 [24]. Until the 1970's Minsky's ideas did not gain a wide degree of interest from his peers, mainly due to lack of light sources with proper parameters and efficient computer units.

The situation changed at the turn of the 1970's and 1980's. In 1979 the Dutch physicist G. F. Brakenhoff (University of Amsterdam) and his team developed the construction of a confocal microscope. Examination of this construction were described in their work [25] and this is where the term "confocal" is defined for the first time. At that time similar research works were also carried out by K. Carlsson's Swedish team (Royal Institute of Technology, Linköping University) [26], R. W. Wijnaendts Van Resandt (EMBL, Heidelberg) [27] and others [28]. The first operating confocal microscopes served as the basis for developing commercial constructions. The latter were introduced onto the market eight years later. One of the first companies which started the production of such microscopes was Lasersharp Ltd., [29]. At the beginning of the 1990's the interest in confocal microscopy increased considerably, mostly due to significant progress in the area of optoelectronics, microelectronics and computer science. New technical possibilities enabled the development of microscopes with more advanced designs that made use of laser radiation as a light source. This is how the new type of classical confocal microscopy was created – confocal laser scanning microscopy [30].

CLSM is one of the most dynamic and rapidly growing microscopic techniques, that has room for a broad array of future developments. Its vast technical possibilities were used in the construction of new advanced 3D laser microscopes produced by a number of world concerns (including Bio-Rad, Carl Zeiss, Keyence, Leica, Olympus, Nikon, Thorlabs). Moreover, the scope of applications of this technique was also significantly expanded. Apart from the classical applications in biological [30, 31] and medical sciences [31-34], CLSM is successfully used in technical sciences such as material [35, 36] and mechanical engineering [37-41].

3. Experimental Procedure

3.1. The main goals of the experiment

The main goal of the experiment undertaken was to analyze the possible application of the CLSM in measuring the GWAS with vitrified bond. The Authors tried to test the offered method to determine its real measurement capabilities in relation to the assessed abrasive tools. An additional goal of the experiment was to test the

computer software used in relation to the program's capabilities, its advantages and disadvantages, as well as the operational intuitiveness.

The experiment was carried out in four steps which included:

Step 1: Selecting and preparing samples for tests.

Step 2: Acquiring images of the active surfaces of selected areas of the grinding wheels.

Step 3: Processing, analysis and visualization of the measurement data.

Step 4: Interpretation of the obtained results.

The measurements were carried out in the Laboratory of Micro- and NanoEngineering at Koszalin University of Technology (Poland) and the Laboratory of Physics, Nanostructures and Technical Applications of Nanotechnology at the Technical University of Ostrava (Czech Republic).

3.2. Characterization of used samples

A set of three samples in the form of small ceramic grinding wheels with microcrystalline sintered corundum grains SGTM were used during the tests. All of the grinding wheels were prepared in the Department of the Fundamentals of Materials Science at the Institute of Mechatronics, Nanotechnology and Vacuum Technique within Koszalin University of Technology. The general characteristics of small ceramic grinding wheels selected for measurements are presented in Table 1.

Table 1. General Characteristics of Grinding Wheels Used in the Experiments.

Sample No.	Technical designation	Characteristics
1	1-35×20×10-SG/F46N7VG	Grinding wheel with microcrystalline sintered corundum grains SG TM No. 46, glass-crystalline bond, hardness class N, structure No. 7. State of the GWAS: after reciprocating grinding of Titanium Grade 2 [®] .
2	1-35×20×10-SG/F46K7VG	Grinding wheel with microcrystalline sintered corundum grains SG TM No. 46, glass-crystalline bond, hardness class K, structure No. 7. State of the GWAS: after dressing
3	1-35×20×10-SG/F46L7VG	Breakthrough of the grinding wheel with microcrystalline sintered corundum grains SG TM No. 46, glass-crystalline bond, hardness class L, structure No. 7.

3.3. Characterization of measuring apparatus

The samples selected for the tests underwent optical measurement. In this case two laser microscopes from the LEXT line – OLS3100 and OLS4000 – by Japanese Olympus were used. They enabled the acquisition of images of the examined abrasive tools surfaces in two modes – microscopic and confocal. The general principle of operation of both microscopes in confocal mode consisted in generating the image from the reflections of the light on the focal plane – upon

which the light was at its most intense. Focusing of the light beams on the examined surface was carried out as a result of a precise displacement of the measurement head in a vertical direction (axis z). The focusing moment was determined through differentiating the changes in the intensity of the light beam reaching the detector through the circular pinhole aperture (CPA). The CPA served two purposes; it enabled the acquisition of the image with the highest depth of focus and contrast and it eliminated the image generated outside the focal plane. The main source of light in both microscopes was a laser diode emitting a light beam from the range of the visible spectrum with wavelengths $\lambda = 408$ nm (OLS3100) and $\lambda = 405$ nm (OLS4000) respectively.

Acquisition of spatial images and maps of the examined surfaces of abrasive tools was related to the procedure of precise scanning point by point in axes x - y . The process of scanning was carried out by a special scanner patented by Olympus. The scanner used the integrated Micro Electro-Mechanical Systems (MEMS). Figure 1 shows a general view of laser measuring microscopes LEXT OLS3100 and LEXT OLS4000, while select parameters are compared in *Appendix A*.

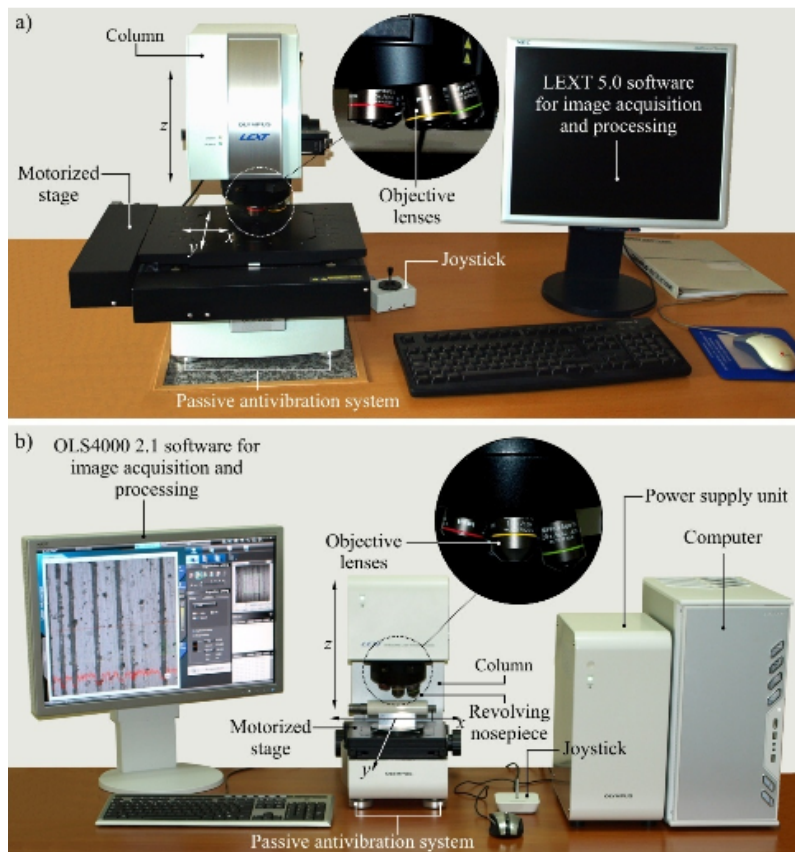


Fig. 1. Two of the 3D Laser Measuring Microscopes, from the Olympus LEXT Series, Used in the Experiments Carried out: a) OLS3100, b) OLS4000.

4. Results and Discussion

This section presents and discusses, in detail, select results of the experimental tests. The parameters of image acquisition acquired during the experiments are included in Table 2.

Table 2. Parameters of Image Acquisition from the Sample Used in Experiments.

Sample No.	Scanning mode	Image size (pixels)	Image size (mm)	Type of objective lens
1*	XYZ step scan + color	4713×2842	11.815×7.121***	MPLFLN5×
2**	XYZ step scan + color	1024×768	2.5×1.9	MPLFLN5×
3**	XYZ step scan + color	1024×768	0.064×0.0075	MPLAPON100×

* sample was measured by OLS4000, ** sample was measured by OLS3100, *** with use of the image stitching procedure

During acquisition of images of the examined surfaces dedicated objective lenses were used, which tend to be the standard for microscopes. Later images were acquired using two types of microscopic lens created by Olympus – MPLFLN and MPLAPON. Their characteristics are presented in Table 3.

Table 3. Selected Parameters of MPLFLN and MPLAPON Objective Lenses Produced by Olympus.

Designation	Mag.	NA	WD (mm)	FN (mm)	Imm.
MPLFLN5*	5×	0.15	20.0	26.5	Dry
MPLAPON100**	100×	0.95	0.35	26.5	–

*M Plan SemiApochromat, **M Plan Apochromat, Mag. – Magnification, NA – Numerical aperture, WD – Working distance, FN – Field number, Imm. – Multi-immersion

The basic software used for acquisition of images and analysis of measurement data were the dedicated OLS 5.0.9 and OLS4100 2.1 programs, that were provided by the producer and came with the microscopes. The above-mentioned programs were supported by advanced TalyMap Platinum 5.0 software, using Mountains Technology™ by French Digital Surf.

In Fig. 2 the results of select analysis of the GWAS No. 1 texture were presented. The GWAS fragment that was the initial aim of the analysis analysis was rather vast.

It covered an area sized 11.815×7.121 mm. Similarly large areas can be obtained using the image stitching procedure. This procedure was discussed in more detail by Kaplonek and Lukianowicz in their work [17]. The area dedicated for analysis was characterized by numerous smears of the intergranular spaces with the machined material chips. In this case it was the alloy Titanium Grade 2®.

The images were acquired using OLS4000 2.1 software. These images are presented below, alongside corresponding results obtained using the TalyMap Platinum 5.0 software (by previously converting the measurement data saved in format *.ols to format *.sur).

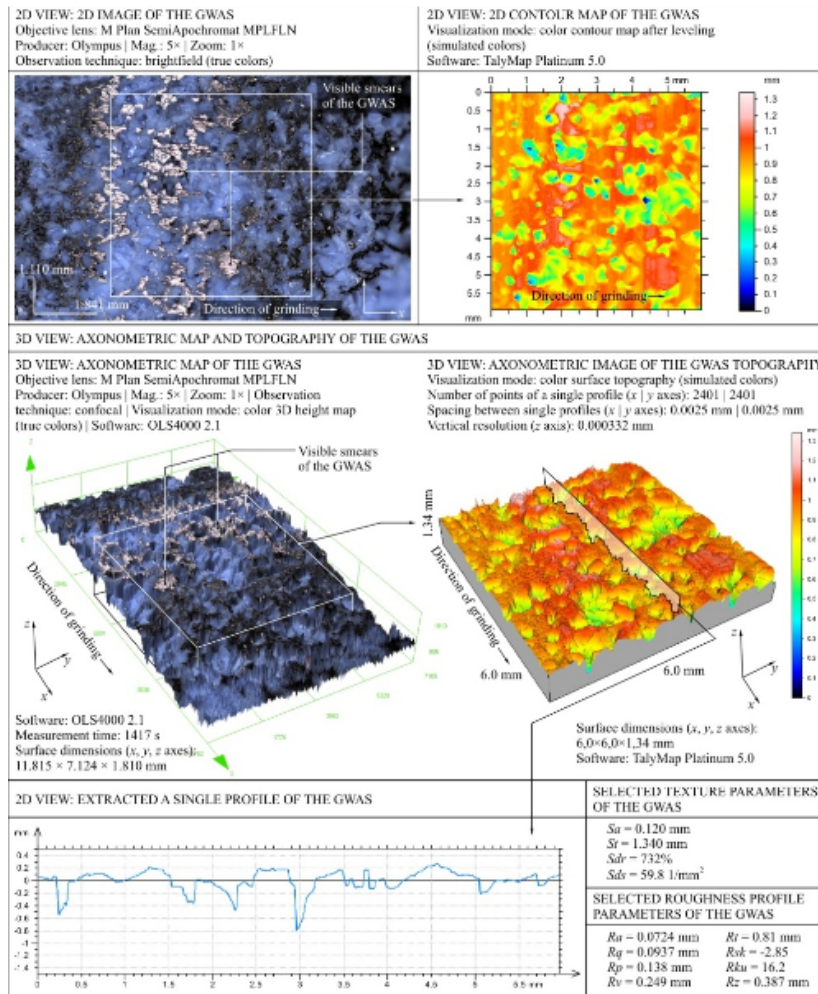


Fig. 2. The Collected Results from the Experiment Carried out on Sample No. 1, Performed in OLS4000 2.1 and TalyMap Platinum 5.0 Software, for Data Obtained Using the 3D Laser Measuring Microscope LEXT OLS4000.

A number of surface roughness parameters were determined on basis of the acquired GWAS topography, and in accordance with [42]. The parameters that turned out to be exceptionally useful in assessment of the degree of smearing were:

- Sdr (developed interfacial area ratio) – hybrid parameter,
- Sds (density of summits of the surface) – spatial parameter.

A comparison of the values of these parameters with the referential values (obtained, among others, from the model sample which may be the surface of the grinding wheel prepared for work) allowed the Authors to draw conclusions about the degree of GWAS wear. Due to the results obtained over a rather short period of time and the lack of a need to prepare samples for measurement, it was

possible to create a core information base on the particular machine process. The information included in such a base can be used in diagnostic systems of machine tools computerized numerical control (CNC).

The analysis of the GWAS condition can also be carried out for a single profile of surface roughness extracted from the surface topography. An example profile is presented in the bottom left part of Fig. 2. This figure clearly demonstrates the gradual blunting of the cutting vertexes as a result of their wear, as well as flattened surface fragments in those places where smears with the machined material occur. Such a quality assessment can be complemented with quantitative assessment on the basis of the determined roughness parameters of the profile.

Figures 3 and 4 present other analyses carried out with OLS4000 2.1 software for sample No. 1. Figure 3 presents the procedure of correcting the 2D map generated for the selected surface fragment of the grinding wheel 1-35×10×10-SG/F46N7VG. The height of subsequent elements of the grinding wheel surface structure were encoded with simulated colors. The map correction was related mainly to removal of the tool surface curvature and improving the gradient of its characteristic elements (abrasive grains). A profile, whose course, before and after the correction, is presented below, was selected from the map located on the left side of Fig. 3.

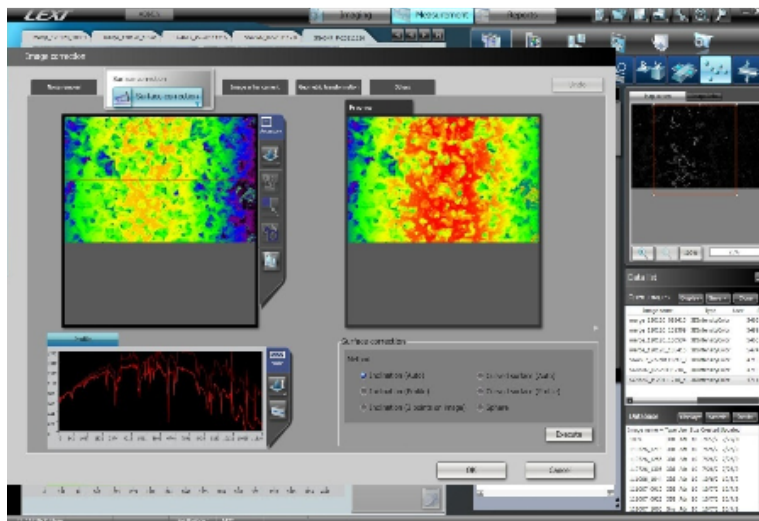


Fig. 3. The Window of OLS4000 2.1 Software during One-Shot Surface Correction Carried out for Sample No. 1.

Figure 4 presents another example analysis carried out with OLS4000 2.1 software for sample No.1. It demonstrates the software capabilities as far as quantitative analyses are concerned. The surface map presents extracted areas of abrasive grains with various heights encoded with simulated colors. For the assumed binarization thresholds, which were respectively: 84.2% and 60.1%, there were three defined areas marked in: yellow (with an average height of 1400 μm), green (with an average height of 1000 μm) and blue (with an average height of 550 μm).

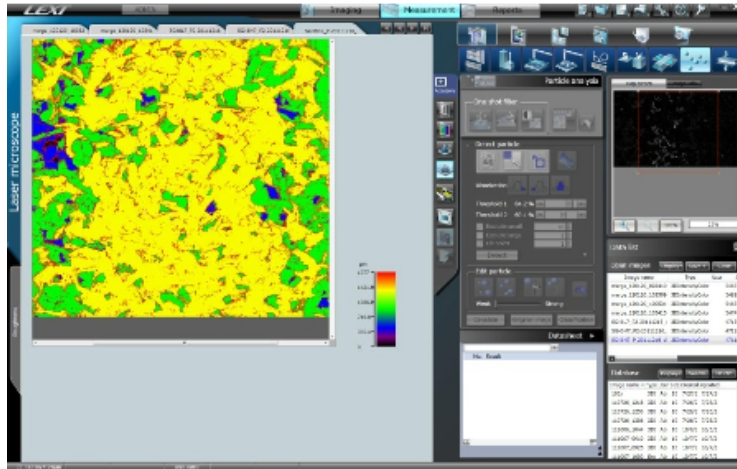


Fig. 4. The Window of OLS4000 2.1 Software during Particle Analysis Carried out for Sample No. 1.

Figures 5 and 6 present the results of the measurements of two fragments from grinding wheel No.2 (1-35×20×10-SG/F46K7VG), whose active surface was shaped in the dressing cut [41]. In order to show the differences in possible analyses of the registered microtopography, the measurements were made with two different values of vertical resolution (axis z), which were respectively: 0.00001 mm (Fig. 5) and 0.015 mm (Fig. 6). At the same time, the remaining parameters were left unchanged (the distance between the single measurement points in axes x - y were 0.0025 mm). When values of the parameters of the examined GWAS structure are compared it can be observed that the change in vertical resolution exerted the greatest influence on the determined density of the surface unevenness vertices.

The value of parameter $Sds = 32.7 \text{ mm}^{-2}$ (Fig. 5) was reduced twice with measurement vertical resolution of 0.015 mm, in comparison to the results obtained with resolution 0.00001 mm ($Sds = 63.2 \text{ mm}^{-2}$, Fig. 6). Taking into consideration the fact that the surface of the same grinding wheel was measured, such a great difference in values results from the decrease in the number of details in the measurements, with the discretization step magnified to 1500 times of axis z , from $0.01 \mu\text{m}$ to $15 \mu\text{m}$. Such a change of measurement conditions enabled almost a twofold reduction in the measurement time. However, the obtained data does not project the assessed surface in a satisfying manner, which is particularly visible on the extracted single GWAS roughness profile (bottom-left of Fig. 6).

Figure 7 presents the differences in imaging of the GWAS fragment sized $4.0 \times 2.51 \text{ mm}$ for sample No.2 using the image acquired with brightfield technique and the confocal image. A comparison of both images makes the observance of details of the geometric structure of the assessed abrasive tools possible (especially the abrasive grains, the bond bridges and participation of the intergranular free spaces). It also allows for extraction of those GWAS fragments upon which various defects were observed (including smears of the surface with machined material). The possibility of obtaining images for a given surface

fragment, using a variety of imaging techniques, is particularly useful – especially due to the thoroughness of its analysis.

In the example presented in Fig. 7, the use of brightfield techniques, Fig. 7(a) to obtain a clearly higher depth of field observation, is demonstrated. This is useful in the analysis of the stereometric structure of the GWAS. Whilst the image obtained with the confocal technique, Fig. 7(b), allows for far easier determination of the highest located abrasive grains (potentially active), which are most likely to participate in the grinding process.

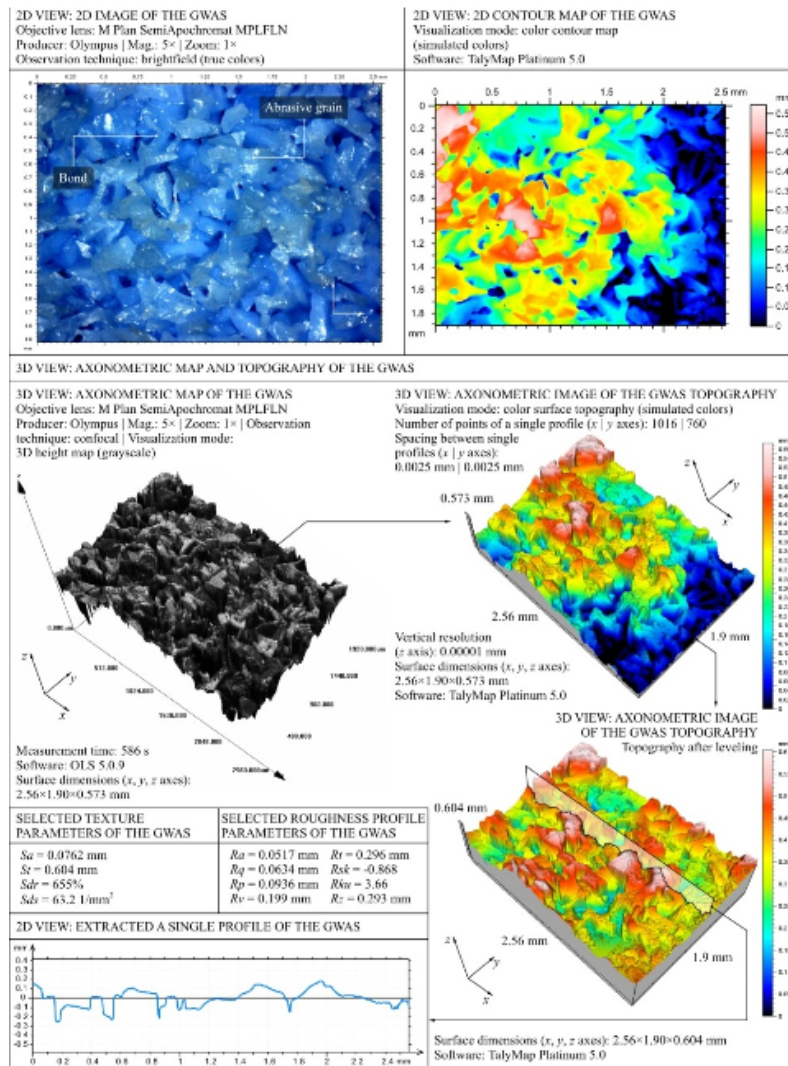


Fig. 5. The Collected Results from the Experiment Carried out on Sample No. 2, Performed in OLS4000 2.1 and TalyMap Platinum 5.0 Software, for Data Obtained Using the 3D Laser Measuring Microscope LEXT OLS4000 with Vertical Resolution (z-axis) 0.00001 mm.

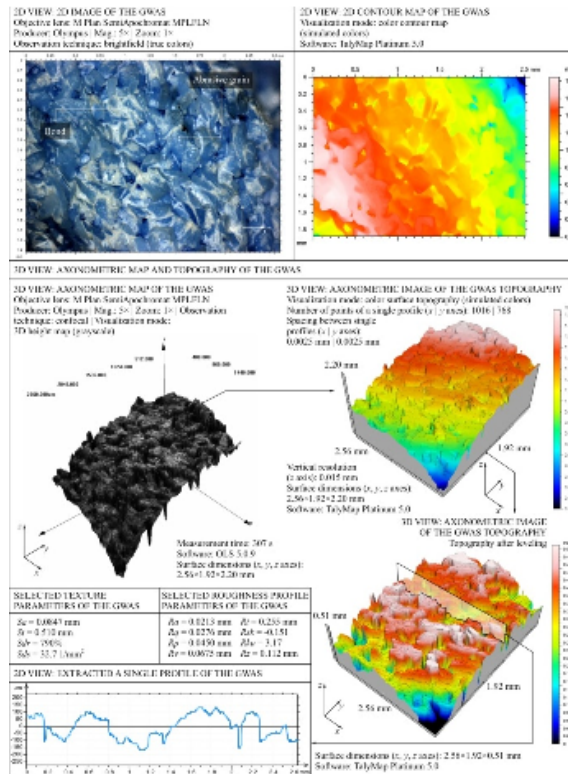


Fig. 6. The Collected Results from the Experiment Carried out on Sample No. 2 Performed in OLS4000 2.1 and TalyMap Platinum 5.0 Software, for Data Obtained Using the 3D Laser Measuring Microscope LEXT OLS4000 with Vertical Resolution (z-axis) 0.015 mm.

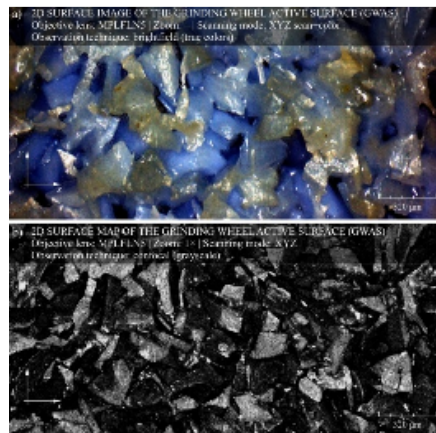


Fig. 7. Differences between (a) Optical Images (Brightfield) and (b) Confocal Images, Obtained Using the 3D Laser Measuring Microscope LEXT OLS3100 for Sample No. 2.

Figure 8 depicts a comparison of selected analyses of the No.3 grinding wheel fracture surface, with a clearly visible glass-crystalline bond bridge. The bridge joins two adjacent microcrystalline sintered corundum grains SGTM.

The high resolution (62.5 nm in axes *x-y*, 50 nm in axis *z*) at which the surface was measured allows for precise assessment of the microcrystalline structure of abrasive grains SGTM. These grains are constructed from submicrocrystals Al₂O₃, which are recognized as microsummits and taken into consideration in the algorithm that determines the value of parameter $Sds = 36220 \text{ mm}^{-2}$. The acquired image also allows for identification of crystalline insertions in the glass mass, which are included in the bond used during the construction of the tool [43].

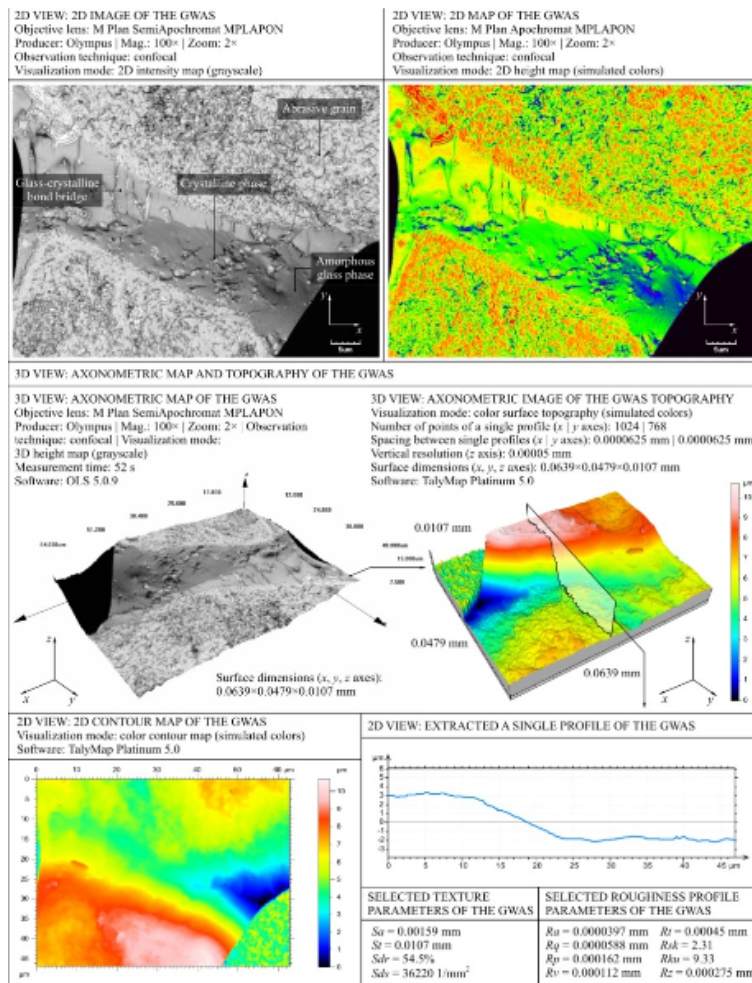


Fig. 8. The Collected Results from the Experiment Carried out on Sample No. 3, Performed in OLS4000 2.1 and TalyMap Platinum 5.0 Software, for Data Obtained Using the 3D Laser Measuring Microscope LEXT OLS4000.

5. Conclusions

This work presents select aspects of the application of one of the new types of classical confocal microscopy, defined as 3D laser microscopy, in the diagnostics of abrasive tools. A set of 3 grinding wheels, made from sintered microcrystalline corundum SG™ bound with glass-crystalline bond, were utilized in the realization of this experiment. Measurements of the GWAS were carried out using advanced laser microscopes LEXT OLS3100 and LEXT OLS4000 by Olympus. Analysis of the measurement results was carried out using the dedicated programs OLS 5.0.9 and OLS4100 2.1, supported by specialist software TalyMap Platinum 5.0. The experiment results obtained enabled the drawing up of the following general conclusions:

- The possibility of using confocal laser scanning microscopy in the diagnostics of abrasive tools was confirmed. It was concluded that this method allowed for the introduction of a thorough analysis of grinding wheels, with particular consideration of the numerous phenomena, at both micro- and macroscale, occurring on their active surfaces. In the former case this may refer to analysis of surface defects (e.g. smearing with machined material), while in the latter case it is with reference to the analysis of the tool's internal structure (e.g. grain-bond connections).
- In relation to the applied measurement apparatus, its high degree of usefulness in measuring the abrasive tools surfaces was proved. What must be stressed is the great precision of the obtained measurement data (resulting high degree of high resolution of both microscopes – approximately 10 nm in axis z and 120 nm in axes x-y), as well as the relatively short measurement time.
- The applied software was characterized by a wide range of possibilities for processing and analyzing the measurement data. What turned out to be of particularly great value was the possibility of converting the data to *.sur files that could be further processed in specialist software, such as TalyMap Platinum 5.0. Another useful procedure was image stitching, which allowed for the acquisition of rather large surface areas (as big as a few mm²) for later analyses.
- 3D laser microscopy is a dynamically developing measurement technique offering vast application possibilities. The measurement data obtained in this way may serve as a supplement or extension of the data obtained with methods typical of such surfaces, such as stylus profilometry, optical profilometry, interferential microscopy.

Acknowledgment

Part of this work was supported by the Polish Ministry of Science and Higher Education under Grant No. N503 214837. The Authors would like to thank Mrs. Daniela Herman, D.Sc, Ph.D., from the Department of the Fundamentals of Material Science in the Institute of Mechatronics, Nanotechnology and Vacuum Technique at Koszalin University of Technology, for preparing the grinding wheels for tests, as well as Mrs. Petra Matejkova, M.Sc., from the Laboratory of Physics, Nanostructures and Technical Applications of Nanotechnology at the Technical University of Ostrava (Czech Republic) and Mr. Robert Tomkowski, M.Sc., B.Sc., from the Laboratory of Micro- and Nanoengineering at Koszalin University of Technology, for the optical measurement of the test samples surface topographies.

References

1. Rowe, W.B. (2009). *Principles of modern grinding technology*. Burlington: William Andrew.
2. Klocke, F. (2009). *Manufacturing Processes 2: Grinding, honing, lapping*. Berlin: Springer-Verlag.
3. Jackson, M.J.; Davis, C.J.; Hitchiner, M.P.; and Mills, B. (2001). High-speed grinding with CBN grinding wheels - Applications and future technology. *Journal of Materials Processing Technology*, 110(1) 78-88.
4. Luetjens, P.; and Mushardt, H. (2004). Grinding out hardened parts. *American Mechanist*, 148(3), 52-59.
5. Richter, A. (2004). Peel out. *Cutting Tool Engineering*, 56(9).
6. Nadolny, K.; Plichta, J.; Herman, D.; Slowinski, B. (2008). Single-pass grinding - An effective manufacturing method for finishing. *Proceedings of the 19th International Conference on Systems Engineering - ICSENG 2008*, 236-241.
7. Tönshoff, H.K.; Karpuschewski, B.; Mandrysch, T.; and Inasaki, I. (1998). Grinding process achievements and consequences on machine tools challenges and opportunities. *CIRP Annals- Manufacturing Technology*, 47(2), 651-668.
8. Marinescu, I.D.; Hitchiner, M.; Uhlmann, E.; Rowe, W.B; and Inasaki, I. (2006). *Handbook of machining with grinding wheels*. (1st Ed.) CRC Press.
9. Malkin, S.; and Guo, C. (2008). *Grinding technology: Theory and applications of machining with abrasives*. New York: Industrial Press Inc.
10. Nadolny, K.; and Slowinski, B. (2011). The effects of wear upon the axial Profile of a grinding wheel in the construction of innovative grinding wheels for internal cylindrical grinding. *Advances in Tribology*, Volume 2011 Article ID 516202, 1-11.
11. Nadolny, K. (2011). Durability of Al₂O₃ grinding wheels with zone-diversified structure in single-pass internal cylindrical grinding. *Advances in Manufacturing Science and Technology*, 35(3), 39-53.
12. Jackson, M.J.; and Davim, J.P. (2010). *Machining with abrasives*. Springer, New York.
13. Byrne, G.; Dornfeld, D.; Inasaki, I.; Ketteler, G.; König, W.; and Teti, R. (1995). Tool condition monitoring (TCM) - The status of research and industrial application. *CIRP Annals - Manufacturing Technology*, 44(2), 541-567.
14. Tönshoff, H.K.; Friemuth, T.; and Becker J.C. (2002). Process monitoring in grinding. *CIRP Annals - Manufacturing Technology*, 51(2), 551-571.
15. Butler, D.L.; Blunt, L.A.; See, B.K.; Webster, J.A.; and Stout, K.J. (2002). The characterisation of grinding wheels using 3D surface measurement techniques. *Journal of Materials Processing Technology*, 127(2), 234-237.
16. Nadolny, K.; Kaplonek, W.; Lukianowicz, Cz.; and Valicek, J. (2011). Laser measurements of surface topography of abrasive tools using Measurement system CLI 2000. *Przegląd Elektrotechniczny (Electrical Review)*, 87(9a) 24-27. (in Polish)

17. Kaplonek, W.; and Lukianowicz, Cz. (2012). *Coherence correlation interferometry* [in] *Surface Topography Measurements, Recent Interferometry Applications in Topography and Astronomy*, Padron, I. (Ed.). Rijeka: InTech.
18. Fujimoto, M.; Ichida, Y.; Sato, R.; and Morimoto, Y. (2006). Characterization of wheel surface topography in cBN grinding. *JSME International Journal Series C*, 49(1), 106-113.
19. Yatsunenko S.; and Fabich M. (2009). 3D laser microscopy for nano-technology and metrology. *Acta Physica Polonica A*, 116(Supplement), S194-S195.
20. Claxton, N.S.; Fellers, T.J.; and Davidson, M.W. (2010). *Laser scanning confocal microscopy*. Available from: <http://www.olympus-fluoview.com/theory/LSCMIntro.pdf>
21. Clarke, A.R.; and Eberhardt, C. (2002). *Microscopy techniques for materials science*. Cambridge/Boca Raton: Woodhead Publishing Limited/CRC Press.
22. Webb, R.H. (1996). Confocal optical microscopy. *Reports on Progress in Physics*, 59(3), 427-471.
23. Minsky, M. (1988). Memoir on inventing the confocal scanning microscope. *Scanning*, 10(4), 128-138.
24. Minsky, M. (1957/1961). Microscopy apparatus. *US Patent* № 3013467.
25. Brakenhoff, G.J.; Blom, P.; and Barends, P. (1979). Confocal scanning microscopy with high-aperture lenses. *Journal of Microscopy*, 117(2), 219-232.
26. Carlsson, K.; Danielsson, P. E.; Lenz, R.; Liljeborg, A.; Majlöf, L.; and Åslund, N.(1985). Three-dimensional microscopy using a confocal laser scanning microscope. *Optics Letters*, 10(2), 53-55.
27. Wijnaendts Van Resandt, R.W.; Marsman, H.J.B.; Kaplan, R.; Davoust, J.; Stelzer, E.H.K.; Stricker, R. (1985). Optical fluorescence microscopy in three dimensions: Microtomoscopy. *Journal of Microscopy*, 138(1), 29-34.
28. Inoué, S. (2006). *Foundations of confocal scanned imaging in light microscopy* [in] *Handbook of Biological Confocal Microscopy* (3rd Ed.), Pawley, J.B. (Ed.). New York: Springer Science+Business.
29. Amos, W.B.; and White, J.G. (2003). How the confocal laser scanning microscope entered biological research. *Biology of the Cell*, 95(6), 335-342.
30. Miller, F.P.; Vandome, A.F.; and McBrewster, J. (2010). *Confocal laser scanning microscopy*. Alphascript Publishing.
31. Buttino, I.; Ianora, A.; Carotenuto, Y.; Zupo, V.; and Miralto, A. (2003). Use of the confocal laser scanning microscope in studies on the developmental biology of marine crustaceans. *Microscopy Research and Technique*, 60(4), 458-464.
32. Kamioka, H.; Honjo, T.; and Takano-Yamamoto, T. (2001). A three-dimensional distribution of osteocyte processes revealed by the combination of confocal laser scanning microscopy and differential interference contrast microscopy. *Bone*, 28(2), 145-149.
33. Scivetti, M.; Pilolli, G.P.; Corsalini, M.; Lucchese, A.; and Favia, G. (2007). Confocal laser scanning microscopy of human cementocytes: analysis of three-dimensional image reconstruction. *Annals of Anatomy - Anatomischer Anzeiger*, 189(2), 169-174.

34. López-Cepero, J.M.; de Arellano-López, A.R.; Quispe-Cancapa, J.J.; and Martínez-Fernández, J. (2005). Confocal microscopy for fractographical surface characterization of ceramics. *Microscopy and Analysis*, 19(5), 13-15.
35. Polansky, R.; Mentlik, V.; Prosr, P.; and Susir, J. (2009). Influence of thermal treatment on the glass transition temperature of thermosetting epoxy laminate. *Polymer Testing*, 28(4), 428-436.
36. Hanlon, D.N.; Todd, I.; Peekstok, E.; Rainforth, W.M.; and van der Zwaag, S. (2001). The application of laser scanning confocal microscopy to tribological Research. *Wear*, 251(1-12), 1159-1168.
37. Ismail, M.F.; Yanagi, K.; and Isobe, H. (2011). Characterization of geometrical properties of electroplated diamond tools and estimation of its grinding performance. *Wear*, 271(3-4), 559-564.
38. Kaplonek, W.; Lukianowicz, Cz.; Nadolny, K.; and Tomkowski, R. (2011). Confocal laser scanning microscopy used for assessment of stereometric features of engineering surfaces. *Measurement Automation and Monitoring*, 57(11), 1409-1413. (in Polish)
39. Nadolny, K.; and Kaplonek, W. (2012). Confocal laser scanning microscopy for characterisation of surface microdiscontinuities of vitrified bonded abrasive tools. *International Journal of Mechanical Engineering and Robotics Research*, 1(1), 15-29.
40. Kaplonek, W.; Tomkowski, R.; and Zelenak, M. (2012). Measurements of surface topography of microfinishing films with use of confocal laser scanning microscopy. *Measurement Automation and Monitoring*, 58(1), 37-39. (in Polish)
41. Nadolny, K.; and Kaplonek, W. (2012). Design of a device for precision shaping of the grinding wheel macro- and microgeometry. *Journal of Central South University of Technology*, 19(1), 135-143.
42. Stout, K.J.; Sullivan, P.J.; Dong, W.P.; Mainsah, E.; Lou, N.; Mathia, T.; and Zahouani, H. (1993). The Development of methods for the characterization of roughness in three dimensions. *Publication No. EUR 15178 EN (Final Report) BCR*, European Community, Brussels.
43. Herman, D. (1998). Glass and glass-ceramic binder obtained from waste material for binding alundum abrasive grains into grinding wheels. *Ceramics International*, 24(7), 515-520.

Appendix A

General Characteristics of 3D Laser Microscopes

**Table A-1. Selected Parameters of
Commercially 3D Laser Microscopes Produced by Olympus.**

Designation	LEXT OLS3000	LEXT OLS3100	LEXT OLS4000
Illumination	Laser $\lambda = 408$ nm + halogen lamp 100W	Laser $\lambda = 408$ nm + halogen lamp 100W	Laser $\lambda = 405$ nm + white LED 30 mW
Revolving nosepiece	Motorised	Motorised	Motorised
Objective lenses	5 \times , 10 \times , 20 \times , 50 \times , 100 \times	5 \times , 10 \times , 20 \times , 50 \times , 100 \times	5 \times , 10 \times , 20 \times , 50 \times , 100 \times
Total magnification	120 \times ~14400 \times	120 \times ~14400 \times	108 \times ~17280 \times
Optical zoom	1 \times –6 \times	1 \times –6 \times	1 \times –8 \times
Resolution	10 nm (z) 120 nm (x-y)	10 nm (z) 120 nm (x-y)	10 nm (z) 120 nm (x-y)
Movement	10 mm (z) 100 \times 100 (x-y)	70 mm (z) 150 \times 100 (x-y)	10 mm (z) 100 \times 100 (x-y)
Height of specimen	100 mm	100 mm	130 mm

**Table A-2. Selected Parameters of
Commercially 3D Laser Microscopes Produced by Keyence.**

Designation	VK-X210	VK-8710	VK-9710 Gen. II
Illumination	Laser $\lambda = 408$ nm + halogen lamp 100W	Laser $\lambda = 658$ nm + halogen lamp 100W	Laser $\lambda = 408$ nm + halogen lamp 100W
Revolving nosepiece	Motorised	Motorised	Motorised
Objective lenses	10 \times , 20 \times , 50 \times , 150 \times	10 \times , 20 \times , 50 \times , 150 \times	10 \times , 20 \times , 50 \times , 150 \times
Total magnification	200 \times ~24000 \times	200 \times ~18000 \times	200 \times ~18000 \times
Optical zoom	1 \times –8 \times	1 \times –6 \times	1 \times –6 \times
Resolution	0,5 nm (z)	1 nm (z)	1 nm (z)
Movement	70 mm (z)	70 mm (z)	70 mm (z)